Eur. Phys. J. D **37**, 283–290 (2006)
DOI: 10.1140/epjd/e2005-00306-3

THE EUROPEAN PHYSICAL JOURNAL D

Continuous variable encoding by ponderomotive interaction

S. Pirandola, S. Mancini, D. Vitali[a], and P. Tombesi

Dipartimento di Fisica, Università di Camerino, via Madonna delle Carceri 9, 62032 Camerino, Italy

Received 21 July 2005
Published online 16 November 2005

Abstract. Recently it has been proposed to construct quantum error-correcting codes that embed a finite-dimensional Hilbert space in the infinite-dimensional Hilbert space of a system described by continuous quantum variables [D. Gottesman et al., Phys. Rev. A **64**, 012310 (2001)]. The main difficulty of this continuous variable encoding relies on the physical generation of the quantum codewords. We show that ponderomotive interaction suffices to this end. As a matter of fact, this kind of interaction between a system and a meter causes a frequency change on the meter proportional to the position quadrature of the system. Then, a phase measurement of the meter leaves the system in an eigenstate of the stabilizer generators, provided that system and meter's initial states are suitably prepared. Here we show how to implement this interaction using trapped ions, and how the encoding can be performed on their motional degrees of freedom. The robustness of the codewords with respect to the various experimental imperfections is then analyzed.

PACS. 03.67.Pp Quantum error correction and other methods for protection against decoherence – 32.80.Lg Mechanical effects of light on atoms, molecules, and ions – 03.65.Ta Foundations of quantum mechanics; measurement theory

1 Introduction

Quantum information, as well as classical information, can be carried either by discrete or continuous variable (CV) systems. The latter have attracted an increasing interest during last years [1]. In particular quantum error correction (QEC) techniques have been extended to this framework in order to allow CV quantum computation [2,3]. However, CV QEC presents some different aspects with respect to that concerning qubits. In fact, while it is reasonable to encode a qubit in a block of qubits using a QEC code protecting against a large error on a single qubit of the block, this is no more true in CV systems. In such a case, in fact, the most probable effect caused by decoherence is a small diffusion in the position and momentum of all the particles. This is just the kind of noise treated in [3] where *shift-resistant* quantum codes for qudits are suitably extended to CV systems. The main drawback of such codes is the preparation of the encoded states which ideally are non-normalizable states and therefore can only be approximated introducing an intrinsic error probability. Travaglione and Milburn [4] have shown that it is possible to generate such approximate states by performing a sequence of operations similar to a quantum random walk algorithm [5]. More recently, we have proposed an all-optical scheme based on the cross-Kerr interaction to realize such a code [6]. In this paper we follow the suggestion of reference [3] and we study a *ponderomotive* interaction [7] to embed a qubit in a CV quantum system.

The paper is organized as follows. In Section 2 we rapidly review some elements from reference [3] and we turn from an ideal situation to a more realistic one. In Section 3 the physical implementation of the CV encoding scheme is proposed. Section 4 is for conclusions.

2 Encoded states

A single qubit living in a Hilbert space $\mathcal{H}$ with basis $\{|0\rangle, |1\rangle\}$ can be encoded into a single oscillator in such a way that the two resulting codewords $\overline{|0\rangle}, \overline{|1\rangle}$ provide protection against small diffusion errors in both position x and momentum p (the quantum operators obey the commutation rule $[\hat{x}, \hat{p}] = i$ so that x, p are dimensionless quantities). The two quantum codewords $\overline{|0\rangle}, \overline{|1\rangle}$ are the simultaneous eigenstates, with eigenvalue $+1$, of the displacement operators $\hat{D}_x(2\theta) = e^{-2i\theta\hat{p}}$, $\hat{D}_p(2\pi\theta^{-1}) = e^{2i\pi\theta^{-1}\hat{x}}$, with $\theta \in \mathbb{R}$, which are also the stabilizer generators of the code [8]. These codewords are therefore invariant under the shifts $x \to x - 2\theta$ and $p \to p - 2\pi\theta^{-1}$. Up to a normalization factor they are

[a] e-mail: david.vitali@unicam.it

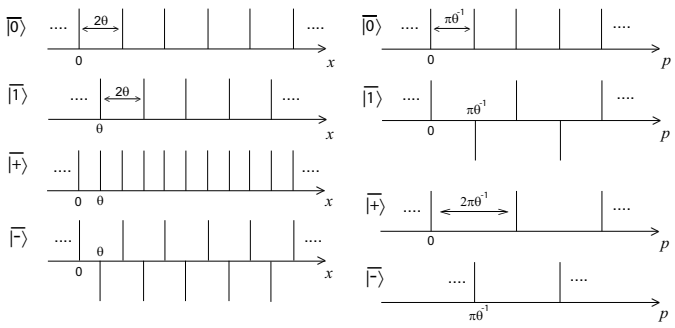

Fig. 1. Ideal encoded states $\overline{|0\rangle}, \overline{|1\rangle}$ ($\bar{Z}$ eigenstates) and $\overline{|+\rangle}, \overline{|-\rangle}$ ($\bar{X}$ eigenstates). On the left the structure of the spatial wavefunctions is displayed while on the right the structure of the momentum wavefunction is displayed. Each spike is ideally a Dirac-delta function.

given by

$$\overline{|0\rangle} = \sum_{s=-\infty}^{+\infty} |x = 2\theta s\rangle = \sum_{s=-\infty}^{+\infty} \left|p = \pi\theta^{-1}s\right\rangle, \qquad (1)$$

$$\overline{|1\rangle} = \sum_{s=-\infty}^{+\infty} |x = 2\theta s + \theta\rangle = \sum_{s=-\infty}^{+\infty} (-1)^s \left|p = \pi\theta^{-1}s\right\rangle = \hat{D}_x(\theta)\overline{|0\rangle}, \qquad (2)$$

i.e. they are a coherent superposition of infinitely squeezed states (position eigenstates and momentum eigenstates). Each of them is a comb-state both in x and in p with equally spaced spikes (2θ in x and $\pi\theta^{-1}$ in p). The codewords $\overline{|0\rangle}, \overline{|1\rangle}$ are also eigenstates of the encoded bit-flip operator $\bar{Z} = \hat{D}_p(\pi\theta^{-1})$. Equivalently one can also choose the codewords $\overline{|\pm\rangle} = [\overline{|0\rangle} \pm \overline{|1\rangle}]/\sqrt{2}$ which are the eigenstates of the encoded phase-flip operator $\bar{X} = \hat{D}_x(\theta)$ and are given by:

$$\overline{|+\rangle} = \sum_{s=-\infty}^{+\infty} |x = \theta s\rangle = \sum_{s=-\infty}^{+\infty} \left|p = 2\pi\theta^{-1}s\right\rangle, \qquad (3)$$

$$\overline{|-\rangle} = \sum_{s=-\infty}^{+\infty} (-1)^s |x = \theta s\rangle = \sum_{s=-\infty}^{+\infty} \left|p = 2\pi\theta^{-1}s + \pi\theta^{-1}\right\rangle. \qquad (4)$$

Also these states are comb-like states both in x and in p, with equally spaced spikes (θ in x and $2\pi\theta^{-1}$ in p). The four codewords states are schematically displayed in Figure 1.

The recovery process is realized by measuring the stabilizer generators $\hat{D}_x(2\theta)$, $\hat{D}_p(2\pi\theta^{-1})$. The measurement of the X-generator $\hat{D}_x(2\theta) = \hat{p}(\mathrm{mod}\pi\theta^{-1})$ reveals momentum shifts Δp which are correctable if $|\Delta p| < \pi\theta^{-1}/2$; in such a case the correction is made by shifting p so to become equal to the nearest multiple of $\pi\theta^{-1}$. In the same way, the measurement of the Z-generator $\hat{D}_p(2\pi\theta^{-1}) = \hat{x}(\mathrm{mod}\theta)$ reveals position shifts which are correctable if $|\Delta x| < \theta/2$; in such a case the correction is made by shifting x so to coincide with the nearest multiple of θ.

Reference [3] proposed the following recipe for the generation of the codeword states.

1. Preparation of a particle in the $p = 0$ eigenstate (i.e. completely delocalized in position).
2. Coupling the particle to a meter (i.e. an oscillator, with ladder operators $\hat{c}$, $\hat{c}^\dagger$) via the non linear interaction $\hat{H}_{NL} = g\hat{c}^\dagger\hat{c}\hat{x}$. This interaction modifies the frequency of the meter by $\Delta\omega = gx$ so that, at time $t = \pi\theta^{-1}g^{-1}$, the phase of the meter is shifted by $\Delta\phi = \pi\theta^{-1}x$.
3. Reading out the phase of the meter $\Delta\phi$ at a time t, i.e. measuring $\hat{x}(\mathrm{mod}2\theta)$. This measurement projects the initial state into a superposition of equally spaced delta function $\delta(x - 2\theta s + \varepsilon)$ with $s = 0, \pm 1, ...$ and $\varepsilon \in \mathbb{R}$.
4. Applying a suitable transformation to obtain any desired encoded qubit state $a\overline{|0\rangle} + b\overline{|1\rangle}$.

Ideally the codewords are non-normalizable states infinitely squeezed both in x and p, but in practice one can only generate states with finite squeezing, i.e. only approximate codewords: $\widetilde{|0\rangle} \sim \overline{|0\rangle}$, $\widetilde{|1\rangle} \equiv \hat{D}_x(\theta)\widetilde{|0\rangle} \sim \overline{|1\rangle}$, $\widetilde{|\pm\rangle} \equiv [\widetilde{|0\rangle} \pm \widetilde{|1\rangle}]/\mathcal{N}_\pm \sim \overline{|\pm\rangle}$ ($\mathcal{N}_\pm$ are normalization constants). For this reason, in order to estimate the *quality* of the encoding scheme, together with the error probability in the recovery process due to the occurrence of an uncorrectable error, we have also to consider the *intrinsic error probability* due to the imperfections of the approximate codewords which can lead to an error even in the presence of a correctable error. Here, we propose a physical implementation of the ideal coding protocol of reference [3], based on the interaction between an atom and a radiation mode. In general, this scheme can be derived from the ideal one by replacing the initial $p = 0$ state with a finitely squeezed state, $\hat{H}_{NL}$ with a ponderomotive interaction, and the phase measurement with a homodyne measurement.

3 Ponderomotive encoding

Our proposal for a physical implementation of the CV encoding scheme is schematically depicted in Figure 2.

We consider a single two-level ion (of mass M and internal transition frequency $\omega_0 = 2\pi c/\lambda_0$) trapped inside a high finesse cavity by a harmonic potential, with trapping frequency ω_a along the direction of the cavity axis x (see Ref. [9] for experimental schemes of this kind). We assume that the trapping potential in the other two directions is steep enough to freeze the motion along y and z. The ion interacts with a single cavity mode with annihilation operator $\hat{c}$ and frequency $\omega_c = 2\pi c/\lambda_c = ck_c$. If the harmonic potential minimum is set halfway in between a node and an antinode of the stationary field of the cavity

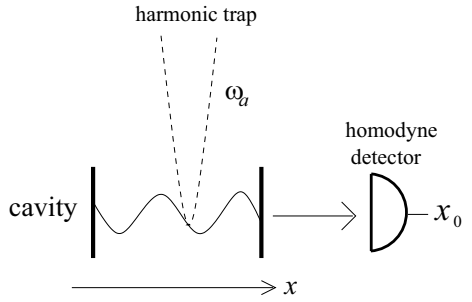

Fig. 2. *Ponderomotive encoding.* An ion is trapped by a harmonic potential within a high finesse cavity, where it interacts with a single mode. After a suitable interaction time, a homodyne measurement of the intracavity quadrature $\hat{X} = (\hat{c} + \hat{c}^\dagger)/\sqrt{2}$ projects the state of the ion onto an approximate comb-like state, i.e. the approximate codeword $\widetilde{|0\rangle}$. A conditional displacement can then be used to generate any correctable state $a\widetilde{|0\rangle} + b\widetilde{|1\rangle}$ (see text).

mode, the ion-cavity Hamiltonian can be written as (assuming, as usual in the optical domain, the rotating wave and dipole approximation)

$$\hat{H} = \hbar\omega_a \hat{a}^\dagger \hat{a} + \hbar\omega_c \hat{c}^\dagger \hat{c} + \hbar\omega_0 \hat{\sigma}_z + \hbar g_0 \left(\hat{\sigma}^\dagger \hat{c} + \hat{c}^\dagger \hat{\sigma}\right) \cos(k_c \hat{x} + \pi/4). \quad (5)$$

In this Hamiltonian $\hat{\sigma}_z = (\hat{\sigma}^\dagger \hat{\sigma} - \hat{\sigma}\hat{\sigma}^\dagger)/2$, $\hat{\sigma}, \hat{\sigma}^\dagger$ are the atomic spin-1/2 operators associated with the two internal levels whose transition is quasi-resonant with the optical cavity mode, $\hat{x} = \sqrt{\hbar/(2M\omega_a)}(\hat{a}+\hat{a}^\dagger)$ is the atomic center-of-mass (CM) position operator, $\hat{c}, \hat{c}^\dagger$ are the cavity mode annihilation and creation operators, and g_0 is the atom-field coupling constant.

A ponderomotive interaction between the atom and the cavity mode is obtained in the dispersive limit in which the cavity mode is highly (red) detuned from the atomic transition. In this limit, the upper atomic level can be adiabatically eliminated and also the spontaneous emission from it can be neglected. In such a condition the atom always remains in its ground state and the resulting ponderomotive Hamiltonian (in interaction picture with respect to $\hat{H}_0 = \hbar\omega_c \hat{c}^\dagger \hat{c}$), is

$$\hat{H} = \hbar\omega_a \hat{a}^\dagger \hat{a} + \hbar \frac{g_0^2}{\delta} \hat{c}^\dagger \hat{c} \cos^2(k_c \hat{x} + \pi/4), \quad (6)$$

where $\delta = \omega_0 - \omega_c$. We then make a second assumption, the Lamb-Dicke limit, which amounts to assume that the ion CM is well localized with respect to a wavelength of the cavity mode λ_c. This assumption allows us to linearize the resulting optical potential in the far-off resonance regime. We thus end up with the simple Hamiltonian [10]

$$\hat{H} = \hbar\omega_a \hat{a}^\dagger \hat{a} - \hbar \frac{g_0^2}{2\delta} \hat{c}^\dagger \hat{c} - \hbar g \hat{c}^\dagger \hat{c} \left(\hat{a} + \hat{a}^\dagger\right), \quad (7)$$

where $g = (g_0^2/\delta)\xi$ and $\xi \equiv k_c \sqrt{\hbar/2M\omega_a}$ is the Lamb-Dicke parameter.

The time evolution operator takes the form [11,12]

$$\hat{U}(\tau) = e^{ik^2 \left(\hat{c}^\dagger \hat{c}\right)^2 (\tau - \sin\tau)} e^{k\hat{c}^\dagger \hat{c}\left(\eta \hat{a}^\dagger - \eta^* \hat{a}\right)} e^{-i\tau \hat{a}^\dagger \hat{a}}, \quad (8)$$

where $\tau \equiv \omega_a t$, $k \equiv g/\omega_a$, $\eta \equiv 1 - e^{-i\tau}$. In writing down equation (8) we have disregarded the free radiation field evolution term.

We now consider as initial condition of the ion-cavity system the tensor product of a coherent state of amplitude α for the cavity mode and a position squeezed state of amplitude β and squeezing parameter $\varepsilon = r \exp\{2i\phi\}$ for the ion center of mass (see Ref. [13] for the preparation of motional squeezed states of the ion CM)

$$|\Psi(0)\rangle = |\beta, \varepsilon\rangle_a \otimes |\alpha\rangle_c, \quad |\beta, \varepsilon\rangle_a = \hat{D}(\beta)\hat{S}(\varepsilon)|0\rangle_a, \quad (9)$$

where $\hat{D}(\beta)$ is the displacement operator and $\hat{S}(\varepsilon)$ is the squeezing operator [14]. In order to compute the time-evolved state $|\Psi(\tau)\rangle = \hat{U}(\tau)|\Psi(0)\rangle$, we expand the optical mode coherent state $|\alpha\rangle_c$ in number states $|n\rangle_c$ and use the Baker-Campbell-Hausdorff expansion [15]. After some algebra, we obtain

$$|\Psi(\tau)\rangle = \frac{1}{\sqrt{\cosh r}} \exp\left[-\frac{\Gamma\beta^{*2} + |\alpha|^2}{2}\right] \times \sum_{n=0}^{\infty} \frac{\alpha^n}{\sqrt{n!}} \exp[\Gamma\beta^* e^{-i\tau}\left(\hat{a}^\dagger - nk\eta^*\right) - (\Gamma/2)e^{-2i\tau}\left(\hat{a}^\dagger - nk\eta^*\right)^2 + ik^2 n^2(\tau - \sin\tau)] \times \left|\beta e^{-i\tau} + nk\eta\right\rangle_a \otimes |n\rangle_c, \quad (10)$$

where $\left|\beta e^{-i\tau} + nk\eta\right\rangle_a$ are coherent states of the ion CM motion and $\Gamma \equiv \exp\{2i\phi\}\tanh r$. Inserting the identity decomposition in the basis of ion CM coherent states, $\hat{I} = \int d^2\gamma |\gamma\rangle_a \langle\gamma| /\pi$ in equation (10), we obtain

$$|\Psi(\tau)\rangle = \mathcal{A} \sum_{n=0}^{\infty} \mathcal{B}_n \int \frac{d^2\gamma}{\pi} e^{\mathcal{C}_{n,\gamma}} |\gamma\rangle_a \otimes |n\rangle_c, \quad (11)$$

where we have defined

$$\mathcal{A} \equiv (\cosh r)^{-1/2} e^{-\frac{\Gamma\beta^{*2} + |\alpha|^2}{2}}, \quad (12)$$

$$\mathcal{B}_n \equiv \frac{\alpha^n}{\sqrt{n!}} e^{ik^2 n^2(\tau - \sin\tau) - \Gamma\zeta_n^*(\beta^* + \zeta_n^*/2) - |\beta + \zeta_n|^2/2}, \quad (13)$$

$$\mathcal{C}_{n,\gamma} \equiv [\Gamma(\beta^* + \zeta_n^*) + \beta + \zeta_n]e^{-i\tau}\gamma^* - (\Gamma/2)e^{-2i\tau}\gamma^{*2} - |\gamma|^2/2, \quad (14)$$

with

$$\zeta_n \equiv nk(e^{i\tau} - 1). \quad (15)$$

At the (scaled) time τ we measure the intracavity quadrature $\hat{X} = (\hat{c} + \hat{c}^\dagger)/\sqrt{2}$ obtaining the result X [16]. As a consequence, the cavity mode is projected onto the corresponding quadrature eigenstate $|X\rangle$, while the ion CM

motion is disentangled from the cavity mode and it is projected onto the state with wave-function

$$\Phi(x) = \frac{N_{X,\tau}}{\pi^{1/4}\sqrt{1-\Gamma e^{-2i\tau}}}\mathcal{A}\sum_{n=0}^{\infty}\langle X\,|n\rangle_c\,\mathcal{B}_n e^{\mathcal{D}_n(x)}, \quad (16)$$

where $N_{X,\tau}$ is a normalization constant, and x now stands for the dimensionless ion CM position, i.e. $x \to x\sqrt{M\omega_a/\hbar}$. Furthermore

$$\mathcal{D}_n(x) \equiv \frac{1}{2}(\Gamma - e^{2i\tau})^{-1}\{(\Gamma + e^{2i\tau})x^2 + [\Gamma(\beta^* + \zeta_n^*) + \beta + \zeta_n][\Gamma(\beta^* + \zeta_n^*) + \beta + \zeta_n - 2\sqrt{2}e^{i\tau}x]\}, \quad (17)$$

with $\langle X|n\rangle_c = \pi^{-1/4}\,(2^n n!)^{-1/2}\,H_n(X)e^{-X^2/2}$, $H_n(X)$ being the nth Hermite polynomial.

3.1 Homodyning with a zero outcome

We have now to determine the conditions under which the general ion CM conditional state of equation (16) becomes a comb-like state which can be taken as approximate codeword state. It is possible to see that one needs to choose $k = 1/2$, that the homodyne measurement has to be performed at the appropriate time $\tau = \pi$, and that initially the ion has to be displaced and squeezed in position, which is achieved if we take β, ε real and positive. To see this we consider a particular example of homodyne measurement outcome, which makes things easier to see, i.e. $X = 0$. In such a case in fact, the property $H_{2m}(0) = (-1)^m 2^m(2m-1)!!$, $H_{2m+1}(0) = 0$ $(m = 0, 1, ...)$ allows to get from (16) the following expression for the ion CM wave-function

$$\varphi(x) \equiv \Phi(x)|_{k=1/2;\tau=\pi;\beta,\varepsilon\geq 0;X=0} = N\sum_{m=0}^{\infty}\nu_m\Omega_m(x), \quad (18)$$

where

$$\nu_m \equiv e^{-\alpha^2/2}\frac{\alpha^{2m}}{(2m)!!}, \quad (19)$$

$$\Omega_m(x) \equiv \frac{e^{r/2}}{\sqrt{\pi}}\exp\left\{-\tfrac{1}{2}e^{2r}\left[x - \sqrt{2}(2m-\beta)\right]^2\right\}, \quad (20)$$

(we have also taken α real and positive) and $N = [\mathcal{P}(X=0)]^{-1/2}$ with

$$\mathcal{P}(X=0) = \frac{1}{\sqrt{\pi}}\sum_{m,m'=0}^{\infty}\nu_m\nu_{m'}e^{-2e^{2r}(m-m')^2} \quad (21)$$

being the probability density corresponding to the outcome $X = 0$ of the homodyne measurement. The state of equation (18) represents, in fact, a superposition of position squeezed states centered in $x = \sqrt{2}(2m-\beta)$, $(m = 0, 1, 2...)$, which is however also a superposition of squeezed states in the momentum space p, as one can verify by computing the Fourier transform

$$\psi(p) = \frac{1}{\sqrt{2\pi}}\int\varphi(x)e^{-ipx}dx = \frac{N}{\sqrt{\pi}}\exp\left[-(r+e^{-2r}p^2)/2\right]\sum_{m=0}^{\infty}\nu_m e^{-i\sqrt{2}p(2m-\beta)} \quad (22)$$

(see Figs. 3c, 3e, 3g). Therefore, also in the present scheme, the homodyne measurement of the cavity mode conditionally generates the desired comb-like state, which we can take as the approximate codeword state $\widetilde{|0\rangle}$. This state depends upon the three dimensionless parameters α, β, and r. The parameter r is obviously responsible for squeezing in x and increases the number of spikes in p (as we can see from Eqs. (20, 22)), while α causes squeezing in p and increases the number of spikes in x. This fact can be seen if we consider the probability to have the m^{th} spike $\Omega_m(x)$ in the wave-function $\varphi(x)$, $P(m) = \nu_m/\sum_{m=0}^{\infty}\nu_m$. In fact one can see that the mean value $\bar{m}$ and its standard deviation Δm are approximately given by

$$\bar{m} \simeq \alpha^2/2, \quad \Delta m \simeq \alpha/\sqrt{2}, \quad (23)$$

implying that the number of spikes in x grows linearly with α. These arguments show that the generated approximate comb-like state approaches the ideal codeword state $|\bar{0}\rangle$ of Section 2 for $\alpha, r \to \infty$ and that we have to take these latter parameters as large as possible. By varying the parameter β instead, one simply shifts the state along x.

Therefore, by comparing with the ideal codeword state of equation (1), we have that the state of equation (18) approximates it (except for an unimportant shift by β) with $\theta = \sqrt{2}$. The approximate codeword $\widetilde{|1\rangle} \equiv \hat{D}_x(-\sqrt{2})\widetilde{|0\rangle}$ is generated by a position shift equivalent to a change of the parameter β, $\Delta\beta = 1$, and which can be again realized by applying a suitable electric field (or laser) pulse (see Ref. [13]). After seeing how the two basis codeword states are generated, let us now see how to generate a generic superposition of the two, $a\widetilde{|0\rangle} + b\widetilde{|1\rangle}$. These superpositions can be generated using conditional displacement schemes analogous to those used, for example, in the manipulation of quantum states of trapped ions [13] and which exploit the coupling of a motional degree of freedom with an internal transition of the ion. Schematically these schemes proceed as follows. The atom is prepared in the tensor product state $\widetilde{|0\rangle} \otimes [a|g\rangle + b|e\rangle]$, where $|e\rangle$ and $|g\rangle$ are two ground state sublevels. Then a laser pulse which is only coupled to $|e\rangle$ is applied to the atom and its intensity is tuned so to give exactly a position shift $x \to x - \sqrt{2}$. In this way the state of the atom becomes $a|g\rangle \otimes \widetilde{|0\rangle} + b|e\rangle \otimes \widetilde{|1\rangle}$. Then a rf pulse resonant with the $e \to g$ transition and transforming $|e\rangle \to (|e\rangle + |g\rangle)/\sqrt{2}$ and $|g\rangle \to (|g\rangle - |e\rangle)/\sqrt{2}$ is applied, so that the state of the atom becomes $[|g\rangle \otimes (a\widetilde{|0\rangle} + b\widetilde{|1\rangle}) + |e\rangle \otimes (b\widetilde{|1\rangle} - a\widetilde{|0\rangle})]/\sqrt{2}$. When the internal state of the atom is measured and it is found equal to $|g\rangle$, the atomic motional state is

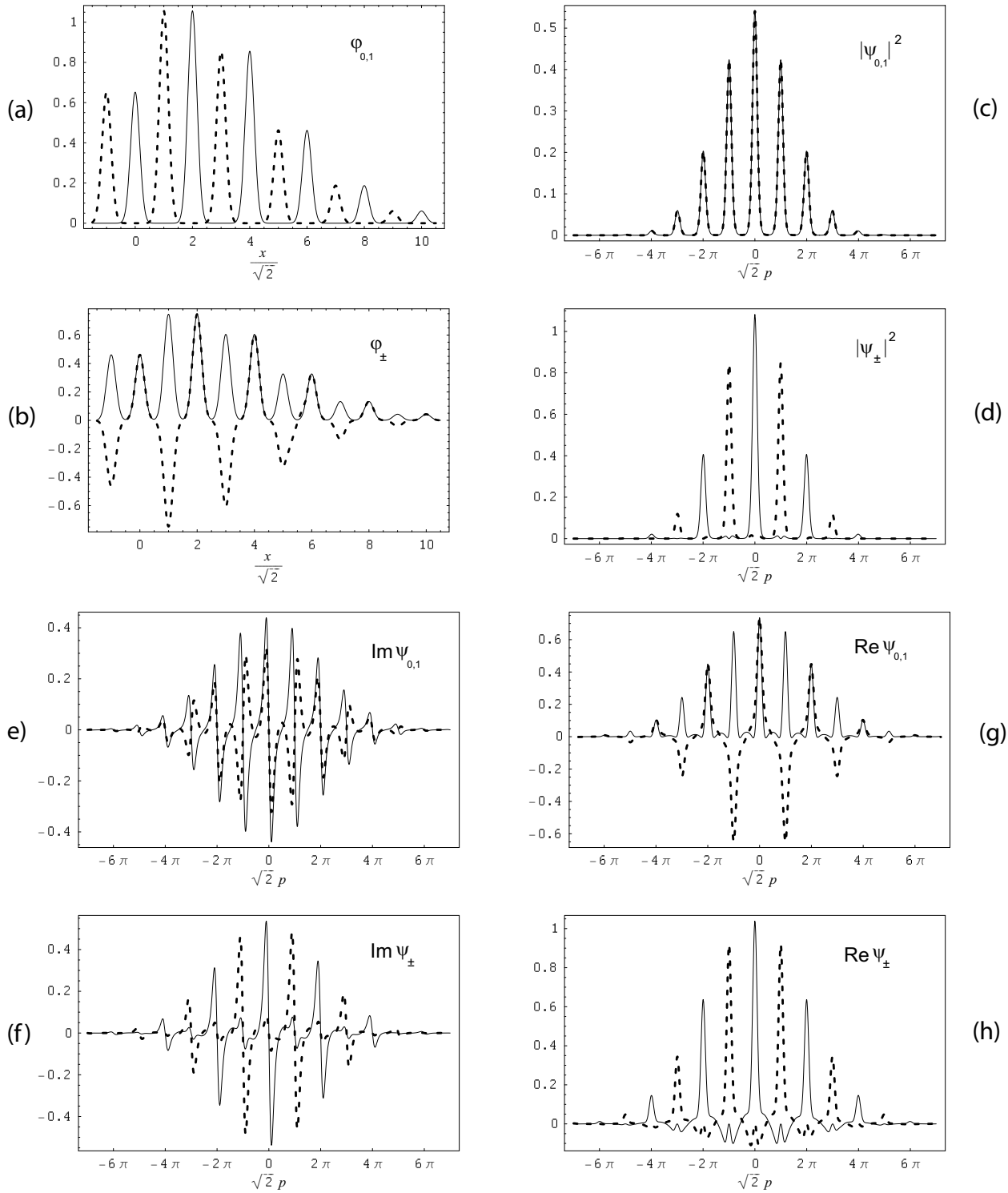

Fig. 3. Plot of the wave-functions in space and momentum coordinates of the approximate codeword states $\widetilde{|0\rangle}$, $\widetilde{|1\rangle}$, $\widetilde{|+\rangle}$ and $\widetilde{|-\rangle}$ for $\alpha = 1.8$, $r = 1.5$ and $\beta = 0$. (a) Spatial wave-functions φ_0 of $\widetilde{|0\rangle}$ (solid line) and φ_1 of $\widetilde{|1\rangle}$ (dashed line) vs. $x/\sqrt{2}$; (b) spatial wave-functions φ_+ of $\widetilde{|+\rangle}$ (solid line) and φ_- of $\widetilde{|-\rangle}$ (dashed line) vs. $x/\sqrt{2}$; (c) momentum probability distributions $|\psi_0|^2$ of $\widetilde{|0\rangle}$ (solid line) and $|\psi_1|^2$ of $\widetilde{|1\rangle}$ (dashed line) vs. $\sqrt{2}p$; (d) momentum probability distributions $|\psi_+|^2$ of $\widetilde{|+\rangle}$ (solid line) and $|\psi_-|^2$ of $\widetilde{|-\rangle}$ (dashed line) vs. $\sqrt{2}p$; (e) imaginary part of the momentum wave-functions Imψ_0 of $\widetilde{|0\rangle}$ (solid line) and Imψ_1 of $\widetilde{|1\rangle}$ (dashed line) vs. $\sqrt{2}p$; (f) imaginary part of the momentum wave-functions Imψ_+ of $\widetilde{|+\rangle}$ (solid line) and Imψ_- of $\widetilde{|-\rangle}$ (dashed line) vs. $\sqrt{2}p$; (g) real part of the momentum wave-functions Reψ_0 of $\widetilde{|0\rangle}$ (solid line) and Reψ_1 of $\widetilde{|1\rangle}$ (dashed line) vs. $\sqrt{2}p$; (h) real part of the momentum wave-functions Reψ_+ of $\widetilde{|+\rangle}$ (solid line) and Reψ_- of $\widetilde{|-\rangle}$ (dashed line) vs. $\sqrt{2}p$.

conditionally generated in the desired encoded superposition $a\widetilde{|0\rangle} + b\widetilde{|1\rangle}$. Particular examples of these superpositions are the eigenstates of the encoded phase-flip operator $\bar{X}$, whose approximate versions are given by $\widetilde{|\pm\rangle} \equiv [\widetilde{|0\rangle} \pm \widetilde{|1\rangle}]/\mathcal{N}_{\pm}$, where $\mathcal{N}_{\pm}^2 = 2[1 \pm \widetilde{\langle 0}|\widetilde{1\rangle}]$ ($\widetilde{|0\rangle}$ and $\widetilde{|1\rangle}$ are not orthogonal in general also in this scheme). It is interesting to notice that the corresponding wave-functions of these latter codeword states $\widetilde{|\pm\rangle}$ in the momentum space are given by

$$\psi_{\pm}(p) \equiv \langle p\,\widetilde{|\pm\rangle} = \pi^{-1/2} N \mathcal{N}_{\pm}^{-1}\; e^{i\sqrt{2}\beta p - (r+e^{-2r}p^2)/2} \times (1 \pm e^{i\sqrt{2}p}) \sum_{m=0}^{\infty} \nu_m e^{-i2\sqrt{2}mp} \quad (24)$$

showing that $|\psi_+(p)|^2$ has spikes at $p_n = \pi(2n)/\sqrt{2}$ while $|\psi_-(p)|^2$ has spikes at $p_n = \pi(2n+1)/\sqrt{2}$ ($n = 0, \pm 1, ...$) (see Fig. 3d). See Figures 3a–3h for plots of the spatial and momentum wave-functions of the various approximate codewords $\widetilde{|0\rangle}, \widetilde{|1\rangle}, \widetilde{|+\rangle}, \widetilde{|-\rangle}$ in the case $\beta = 0$ and for the particular values $\alpha = 1.8$ and $r = 1.5$.

3.2 Intrinsic error probability

As discussed in Section 2, when approximated codewords are used, one has additional errors (intrinsic errors). In fact, due to the presence of the tails of the peaks, the recovery process may lead sometimes to a wrong codeword. The recovery in the spatial variable is performed by measuring the operator $(\hat{x} + \beta\sqrt{2})(\mathrm{mod}\sqrt{2})$. An intrinsic error in the recovery process occurs when, given the state $\varphi_0(x) \equiv \langle x\,\widetilde{|0\rangle}$, the measurement gives a result within one of the error regions: $R_n \equiv \sqrt{2}\,[2n - 3/2 - \beta, 2n - 1/2 - \beta]$, $n = 0, 1...$ The corresponding intrinsic error probability $P_{x,0}$ is equal to the one, $P_{x,1}$, which we would obtain starting from the state $\varphi_1(x) \equiv \langle x\,\widetilde{|1\rangle}$ and considering the complementary error region. So we simply have

$$P_x = \sum_{n=0}^{\infty} \int_{\sqrt{2}(2n-\frac{3}{2}-\beta)}^{\sqrt{2}(2n-\frac{1}{2}-\beta)} dx\,|\varphi_0(x)|^2 . \quad (25)$$

It is possible to prove that, under the condition $r \gtrsim 3/2$, allowing us to use the asymptotic expansion of the error function $\int_x^{+\infty} dt e^{-t^2} = (2x)^{-1} e^{-x^2}[1 - O(x^{-2})]$, we can write the following upper bound for P_x:

$$P_x \lesssim \frac{N^2}{\pi\sqrt{2}} e^{-(r+e^{2r}/2)} [e^{-\alpha^2} + \sum_{m=1}^{\infty} (\nu_{m-1} + \nu_m)^2] . \quad (26)$$

The recovery in the momentum space is instead performed by measuring the operator $\hat{p}(\mathrm{mod}\pi/\sqrt{2})$. An intrinsic error in the recovery process occurs when, given the state $\psi_+(p)$, the measurement gives a result within one of the error regions $R_n^+ \equiv (\pi/\sqrt{2})\,[2n + 1/2, 2n + 3/2]$ for integer n, or, given the state $\psi_-(p)$, the measurement gives a result within one of the error regions $R_n^- \equiv (\pi/\sqrt{2})\,[2n - 1/2, 2n + 1/2]$ for integer n. The corresponding intrinsic error probabilities are given by

$$P_{p,\pm} = \sum_{n=-\infty}^{+\infty} \int_{R_n^{\pm}} dp\,|\psi_{\pm}(p)|^2 . \quad (27)$$

Inserting equation (24) into equation (27) we get, after some algebra,

$$P_{p,\pm} \simeq \frac{2}{\pi} \frac{N^2}{\mathcal{N}_{\pm}^2} e^{-r} \left[K_{0,0}^{\pm} \sum_{m=0}^{\infty} \nu_m^2 + 2 \sum_{m>m'=0}^{\infty} \nu_m \nu_{m'} K_{m,m'}^{\pm} \right], \quad (28)$$

where

$$K_{m,m'}^{\pm} \equiv \sum_{n=-\infty}^{+\infty} \int_{R_n^{\pm}} dp\; \exp(-e^{-2r}p^2) \times (1 \pm \cos\sqrt{2}p) \cos[2\sqrt{2}p(m - m')]. \quad (29)$$

To estimate the quality of the overall encoding procedure provided by this scheme, we have to consider a mean intrinsic error probability $\bar{P}_e$, which is obtained, in general, by averaging over all the possible encoded qubit states. Using the above definitions, we have that the mean intrinsic error probability $\bar{P}_e$ satisfies the inequality

$$\bar{P}_e \lesssim \max\{P_x, P_{p,+}, P_{p,-}\} \equiv P_{\max}, \quad (30)$$

which defines the maximum intrinsic error probability $P_{\max}$, providing therefore a good characterization of the proposed encoding scheme. However, in the considered physical configuration, in a large and significant region of parameters, it is $P_{p,+} \simeq P_{p,-} \equiv P_p \gg P_x$ so that we can take as upper bound for $\bar{P}_e$ simply the quantity P_p.

Let us therefore study the behavior of this upper bound for the intrinsic error probability in the case of system parameters corresponding to a typical experimental cavity QED situation. As we have seen, the amplitude α of the cavity mode coherent state and the squeezing parameter r the ion CM position are the relevant parameters to study, and they should be as large as possible. However, as in the preceding scheme, we have derived our approximate codeword states by making some assumptions and therefore α and r cannot be freely chosen. A first limitation comes from the Lamb-Dicke limit. In practice this implies that during all the process of generation of the comb-like state the ion has to remain localized within a region smaller than λ_c so that the linearization of the optical potential is valid. We can roughly impose $|\bar{x} \pm \Delta x| \lesssim \lambda_c/8$, where $\bar{x}$ is the ion mean position and Δx is its mean position spread. Using equations (18–20,23), we can see that the ion comb-like state $\varphi(x)$ is substantially confined in the interval $\sqrt{2}[2m_- - \beta, 2m_+ - \beta]$, where $m_{\pm} \equiv \max(\alpha^2/2 \pm \alpha/\sqrt{2}, 0)$. Using this fact, we can see that the Lamb-Dicke limit implies

$$(2m_+ - \beta)\frac{2\xi}{k_c} \leq \beta \frac{2\xi}{k_c} \leq \frac{\lambda_c}{8}, \quad (31)$$

which is equivalent to require

$$\beta \leq \frac{\pi}{8\xi} \equiv \beta_{\max}, \alpha \leq \frac{\sqrt{1+4\beta}-1}{\sqrt{2}} \equiv \alpha_{\max}(\beta). \quad (32)$$

In order to reach the maximum value of α we choose $\beta = \beta_{\max}$ so that

$$\alpha \leq \alpha_{\max}(\beta_{\max}) = \frac{\sqrt{1+\pi/(2\xi)}-1}{\sqrt{2}} \equiv \alpha_{\max}. \quad (33)$$

Therefore we have found an "optimal" value β_{max} for β, and a corresponding upper bound α_{max} for α imposed by the adoption of the Lamb-Dicke approximation. Moreover the Lamb-Dicke limit has to be satisfied also by the ion CM state at the beginning, and this implies a condition on the squeezing parameter r which is roughly given by $r > 3/2$.

Finally, the large detuning approximation imposes another limitation on α. In fact, this condition reads $\alpha \lesssim \delta/2g_0$ and using the condition for having a comb-like state $k = 1/2$, implying $\delta = 2\xi g_0^2/\omega_a$, we get

$$\alpha \leq \alpha'_{\max} \equiv \sqrt{\frac{\hbar}{20M\omega_a^3}} g_0 k_c. \quad (34)$$

To summarize, the adopted approximations imply the conditions $r \gtrsim 3/2$, $\alpha \leq \alpha''_{\max} \equiv \min(\alpha_{\max}, \alpha'_{\max})$ and $\beta = \beta_{\max}$.

However, despite these constraints, one can find suitable values, for α and r, such that these bounds are satisfied and a low value for the estimated intrinsic error probability is achievable.

We have done a numerical study of $P_x, P_{p,+}, P_{p,-}$ in the interval $0 \leq \alpha \leq 5.5$ and for $r = 1.5, 2, 3$. As anticipated above it is $P_x \ll P_p \simeq P_{p,+}, P_{p,-}$ so that the intrinsic error probability is practically determined by P_p. This upper bound P_p weakly depends on r and, in fact, it has the same behavior for $r = 1.5, 2, 3$, while it has a significant dependence upon α. As expected, one has better results for increasing α (see Fig. 4), even though one cannot take too large values for it because of the Lamb-Dicke and large detuning approximations employed here.

For example, considering the case of a trapped Ca^+ ion (with $\lambda_0 \simeq 866$ nm), if we choose experimentally realistic values such as $\omega_a \simeq 400$ KHz and $g_0 \simeq 3.8$ MHz, from equations (33, 34) one gets $\alpha''_{\max} \simeq 1$ corresponding to $\beta = \beta_{\max} \simeq 1.2$. In correspondence of these values for α and β, and choosing $r = 1.5$ one has a mean intrinsic error probability $\bar{P}_e \lesssim 9\%$, as we can see from Figure 4. These particular values of α and r imply a *success probability* $\mathcal{P}(X = 0) \simeq 26\%$ according to equation (21). Note that, thanks to its exponential-decaying behavior, the value of the intrinsic error probability can rapidly be improved by accessing stronger ponderomotive interactions (i.e., higher g_0-couplings).

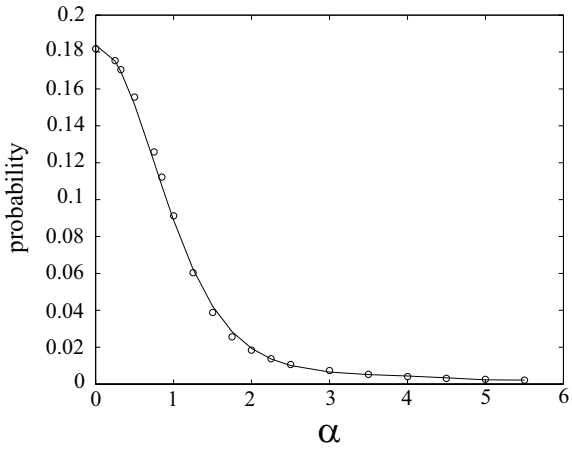

Fig. 4. Upper bound P_p for the mean error probability $\bar{P}_e$ as a function of α in the interval $0 \leq \alpha \leq 5.5$ and for $r = 1.5$ (the curve is indistinguishable from those corresponding to $r = 2$ and $r = 3$). Numerical data (circles) are fitted by an exponential curve (line).

4 Conclusion

For any quantum information processing to become a reality the task of providing adequate error correction needs to be fulfilled. As the quantum mechanical oscillator is a simply and prevalent model in the study of quantum mechanics, it appears to be a natural test bed for such purposes. Thus we have discussed how to embed a qubit in a continuous quantum system, so that its redundancy can be used to correct errors which arise from unwanted interactions with the environment. In particular we have shown that ponderomotive interaction suffices to this end and we have proposed a physical scheme in which a trapped ion within a cavity is considered.

In this configuration, we are able to show that sufficiently low values of the intrinsic error probability are reachable so that idealized states [3] can be effectively engineered with current technology. For the sake of simplicity, throughout the paper we have considered protocols conditioned to a given result of a homodyne measurement of the intracavity field (the case corresponding to the outcome $X = 0$ to be specific). However in practical situations one has to consider a finite interval of acceptable measurement results. Then, it is possible to see that the success probability is improved by enlarging the interval at expenses of an increased error probability.

References

1. See e.g. *Quantum Information Theory with Continuous Variables*, edited by A.K. Pati, S.L. Braunstein (Kluwer Academic Press, 2002)
2. S. Braunstein, Phys. Rev. Lett. **80**, 4084 (1998); S. Lloyd, J.E. Slotine, Phys. Rev. Lett. **80**, 4088 (1998)
3. D. Gottesman, A. Kitaev, J. Preskill, Phys. Rev. A **64**, 012310 (2001)
4. B.C. Travaglione, G.J. Milburn, Phys. Rev. A **66**, 052322 (2002)
5. B.C. Travaglione, G.J. Milburn, Phys. Rev. A **65**, 032310 (2002)
6. S. Pirandola, S. Mancini, D. Vitali, P. Tombesi, Europhys. Lett. **68**, 323 (2004)

7. S. Mancini, P. Tombesi, Phys. Rev. A **49**, 4055 (1994)
8. D. Gottesman, Phys. Rev. A **54**, 1862 (1996); A.R. Calderbank, E.M. Rains, P.W. Shor, N.J.A. Sloane, Phys. Rev. Lett. **78**, 405 (1997)
9. G.R. Gunthorlein et al., Nature **414**, 49 (2001); A.B. Mundt et al., Phys. Rev. Lett. **89**, 103001 (2002)
10. S. Mancini, D. Vitali, P. Tombesi, Phys. Rev. A **61**, 053404 (2000)
11. S. Mancini, V.I. Man'ko, P. Tombesi, Phys. Rev. A **55**, 3042 (1997)
12. S. Bose, K. Jacobs, P.L. Knight, Phys. Rev. A **56**, 4175 (1997)
13. D. Leibfried, R. Blatt, C. Monroe, D. Wineland Rev. Mod. Phys. **75**, 281 (2003)
14. D.F. Walls, G.J. Milburn, *Quantum Optics* (Springer, Berlin, 1994)
15. R.M. Wilcox, J. Math. Phys. **8**, 962 (1967)
16. It is possible to make a direct and precise measurement of this intracavity quantity using a high finesse cavity whose input-output mirror transmittivity is controlled through fast electronic. See for instance: M.S. Taubman, H.M. Wiseman, D.E. McClelland, H.A. Bachor, J. Opt. Soc. Am. B **12**, 1792 (1995)